



SPATIO–TEMPORAL ANALYSIS OF SPECTRAL INDICES AND IN-SITU EDAPHIC SALINITY ESTIMATION IN THE DELTAIC ECOSYSTEM OF INDIAN SUNDARBANS

Priyanka Das¹, Aditi Sarkar², Pabitra Banik^{3*}, Michael A. Powell⁴, and Krishna Chandra Rath⁵

¹ Agricultural and Ecological Research Unit, Indian Statistical Institute, Kolkata, India.

² CAD Centre, Jadavpur University, Kolkata, India.

^{3*} Agricultural and Ecological Research Unit, Indian Statistical Institute, Kolkata, India.

⁴ Dept of Renewable Resources, University of Alberta, Alberta, Canada.

⁵ Department of Geography, Utkal University, Bhubaneswar, Odisha, India.

*Corresponding Author: banikpabitra@gmail.com

ABSTRACT

The Sundarbans area represents the world's most extensive mangrove forests, formed by the confluence of the Ganga-Brahmaputra Rivers delta spread across 10000 km². The significance of the area was recognised by the United Nations Educational, Scientific and Cultural Organization (UNESCO) in 1987 when it was named a World Heritage Site. Past research has demonstrated that mangrove ecosystems are highly susceptible to climate change. The current study explores the relationship between different spectral indices derived from remote sensing using Landsat satellite's Multispectral Scanner (MSS), Thematic Mapper (TM), and Operational Land Imager (OLI) images as indicators of mangrove conditions. Specifically, this study analyses changes in the Normalized Difference Salinity Index (NDSI), the Normalized Difference Vegetation Index (NDVI), and the Land Surface Temperature (LST) index across the Sundarbans from 1972 to 2022. The index values for NDSI positively correlate with measured soil electrical conductivity (EC). The results show that NDVI declined while NDSI and LST increased during the study period. Over the last 50 years (1972-2022), the maximum NDVI values have decreased by 0.54, while the maximum NDSI has increased by 0.7. LST rose by about 0.9 °C between 1995 and 2022. The changes in these indices help identify potential safeguard measures to protect the fragile ecosystem, which help policies related to sustainable mangrove management in the Sundarbans.

Keywords: Land Surface Temperature, Mangrove, NDVI, NDSI, Sundarbans

1. INTRODUCTION

The Sundarbans is the world's largest coastal deltaic mangrove ecosystem and represents a susceptible area in terms of vulnerability to climatic change due to the intricate blend of estuarine and coastal environments (International Union for Conservation of Nature, 2010; Sievers et al., 2020). Moreover, the dynamic relationships between terrestrial and meteorological systems make them highly vulnerable to the effects of climate change.

Plenty of previous research works have documented significant destruction of mangroves. Mitra et al. (2009) observed that the intensity of climate change's impact on the Sundarbans' mangrove forests exceeds the global average, i.e., 0.5 °C increase in surface temperature per decade. According to the U.N.'s Intergovernmental Panel on Climate Change (IPCC, 2013), the average global temperature is predicted to increase by up to 4.8° C by 2081–2100 relative to the 1986–2005 average. Over the past 30 years (1978-2008), the atmospheric temperature is estimated to have risen by 6.14 percent and 6.12 percent in the western and eastern sides of the Sundarbans, respectively. Both sides constitute an average annual increase of approximately 0.05°C yearly (Mitra et al., 2009). Increasing temperatures globally can result in a rise in sea levels (Thomas et al., 2014). A recent study estimates that the current rate of mangrove destruction globally is about 1-2% per year, especially due to rising sea levels (Alongi, 2015). The changing climate will likely generate more harsh effects, such as increased intensity and frequency of extreme floods, storm surges, and cyclones.

There are studies that have emphasised the ecological conditions of the Sundarbans using remote sensing and field data. Remote Sensing (RS) techniques have enhanced the capacity of researchers to provide a complete picture of inaccessible regions of the mangrove ecosystem. However, it is necessary to compare the satellite-derived spectral indices with the field measurements to accurately quantify and assess their ability to monitor and map the variables. In 2018, Deng et al. (2018) studied remote sensing combined with regression to analyse the impact of land-use change on Land Surface Temperature (LST) and Normalized Difference Vegetation Index (NDVI). Thakur et al. (2020) studied the impact of changing land use patterns on the LST and NDVI from 2000 to 2017 and found that the LST is an essential function of LULC. LST has been used mainly to show changes in temperature in urban areas. However, the LST application has recently broadened to include other areas, such as climate change on inland water bodies, crop management, water management, fire monitoring, and geological processes.

Several studies have examined the anthropogenic changes that are influencing different aspects of the Sundarbans' ecology, morphology, land use pattern (Ganguly et al., 2006; Hajra et al., 2017), mangrove loss (Mondal et al., 2018), and tidal channels (Ghosh et al., 2018) over the period. Soil salinity plays a vital role in defining the distribution of mangrove species in the Sundarbans. Soil salinization is also a root cause of soil degradation. The comprehensive literature review indicates limited studies evaluating salinity variation and its linkage with other image-based indicators in the Sundarban regions. Analyzing the Normalized Difference Salinity Index (NDSI) with the soil electrical conductivity (EC) can provide a more substantial basis for updating the variations in salinity across inaccessible areas of the Sundarbans over time.

Improved documentation of ongoing changes in inhabited regions of the Sundarbans and a better understanding of the relationship between changes in soil salinity, soil electro-conductivity, land surface temperature vegetation, and similar environmental indicators will provide insights helpful in identifying ways to reduce future changes and improve the resilience of the Sundarbans' mangroves. The present research is intended to meet the primary objectives of 1) evaluating the broader ecosystem health in the Sundarbans through the spectral-based environmental indicators of mangroves, 2) enhancing the understanding of the spatial and temporal variations of spectral-based environmental indicators (i.e., NDVI, NDSI, and LST), and 3) examining the relationships between indicators (LST, NDSI, NDVI, soil EC) in Sundarbans mangroves.

2. STUDY AREA

Approximately 60% of the Sundarbans lie in Bangladesh, and the balance lies in India (Kundu et al., 2020) (Figure 1). The Sundarbans Biosphere Reserve (SBR) is segmented into a transition zone, a buffer zone, and a core zone. The Sundarbans landscape can be categorized by the different land features, i.e., sandy beaches, mud flats, coastal dunes, estuaries, creeks, inlets, and mangrove swamps. There are roughly 100 low-lying islands in the Indian part of the Sundarbans (the exact number varies over time due to the formation and inundation of smaller islands due to tidal flows and cyclones), and 50% are inhabited. These islands lie on marshy alluvial plains that undergo constant transformation due to siltation, flooding, cyclones, and tidal currents.

The Sundarbans experience a monsoon/rainy season with moderate temperatures throughout the year due to their proximity to the Bay of Bengal and the Indian Ocean. The Sundarbans suffer from frequent storms (cyclones or tropical depressions) between mid-March and November; major cyclones have caused extensive damage to the area (Kar et al., 2015).

Agriculture and fishing are principal sources of livelihood for households in this low-lying region. The mangrove forests of the Sundarbans also play an essential role in the livelihoods of households, such as fishing, logging, and gathering other resources for sale (e.g., honey and beeswax, Keora fruits, medicinal plants). In recent years, tourism has grown in the Sundarbans, providing residents with new opportunities to improve their livelihoods and raise their economic status. These activities, as well as the construction of water management infrastructure in the upstream regions, have profoundly affected water flow and the health of the mangroves in the Sundarbans, especially in the western area of the Indian Sundarbans (Rahman et al., 2011).

3. DATA AND METHODOLOGY

The primary data sources were optical satellite images from Landsat MSS, TM, and OLI sensors. Images were used to define and characterize mangrove areas and to record environmental indicators and their change in the Sundarbans. The spectral indices such as

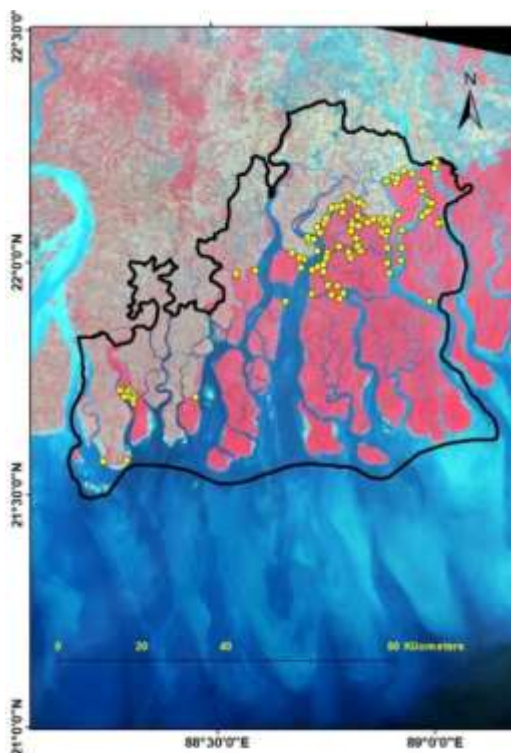


Figure 1. Delineation of the study area (Indian Sundarbans) and distribution of soil sampling sites

NDVI, NDSI, and LST were estimated for 1972, 1995, 2019, and 2022. In addition, soil samples were collected, and the EC of the soils was analysed. Garmin GPS, with an accuracy of ± 5 meters, was used to geo-locate places where soil samples were collected. Subsequently, the statistical interpretation based on the Coefficient of Determination was calculated among the spectral indices and EC variables. Besides that, spatial and temporal variations in the spectral indices were also analysed simultaneously. A brief methodological flowchart is provided in Figure 2. Detailed methodology is discussed in the following subsections.

3.1 Satellite Data and Spectral Indicators

The Landsat series images such as MSS, TM, and OLI were obtained (tiff format) from the United States Geological Survey (USGS) Global Visualization Viewer (GLOVIS) website (Table 1). Erdas Imagine (version 9) and ArcMap (version 10) were used for image processing, spatial database creation, and data analyses. Images covered by water were excluded from the analysis. Spectral radiance values were used to retrieve land surface temperatures from Landsat TM 5, OLI 8, and OLI 9. The LST was extracted from the thermal band using band 6 of Landsat TM and bands 10 and 11 of Landsat 8 and 9.

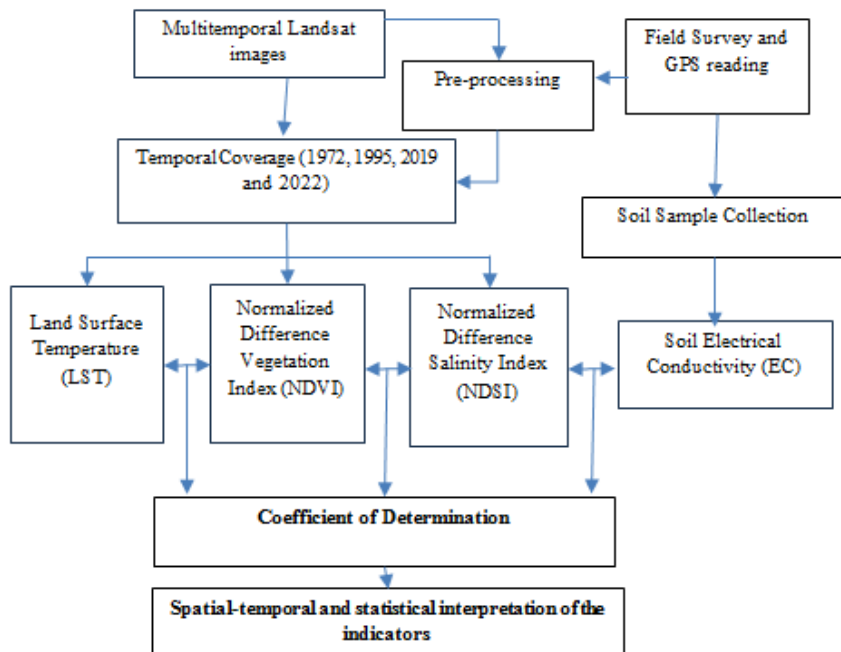


Figure 2. Methodological Flowchart

Table 1. Details of optical satellite images used in this study

DATA	BANDS	SENSOR (LANDSAT)	DATA FORMAT	ACQUISITION DATE	PATH ROW	SPATIAL RESOLUTION
Landsat 1	4	MSS	GEOTIFF	1972-11-05	P148/r45	60 m
Landsat 5	7	TM	GEOTIFF	1995-01-28	P138/r45	30 m
Landsat 8	11	OLI	GEOTIFF	2019-01-30	P138/r45	30 m
Landsat 9	11	OLI	GEOTIFF	2022-12-16	P138/r45	30 m

3.1.1 Generating Spectral Indicators: NDVI, NDSI, and LST

The Normalized Difference Vegetation Index was calculated using data from the Landsat Series according to Equation 1. The NDVI index is based on remotely sensed differences between vegetation's reflectance and absorption bands. High positive NDVI values (near +1) indicate healthy vegetation, while the lowest values (near zero) indicate a lack of vegetation. The steps mentioned in Jeevalaxhmi (2017) were followed to extract NDVI from the satellite images.

$$NDVI = (NIR - R)/(NIR + R) \tag{1}$$

Where NIR = Near Infrared band, R = Red band.

The spectral soil reflectance is influenced by the physical and chemical properties of the soil (e.g., types of salt found in the soil as well as levels of soil moisture, colour, and surface texture). It is well captured by the NIR region of the electromagnetic spectrum. The Normalized Difference Salinity Index (NDSI) is commonly used to record soil salinity fluctuations spatially and temporally; Landsat images (1972, 1995, 2019, and 2022) were used to derive the spectral-based salinity index based on Equation 2. NDSI values range between -1 to +1, where higher values indicate higher salinity.

$$NDSI = (R - NIR)/(R + NIR) \quad (2)$$

Where NIR = Near Infrared band, R = Red band.

Estimates of land surface temperatures were derived from geometrically corrected Landsat TM and OLI images. The split window method and the spectral radiance model were used to retrieve surface temperature using the thermal bands of Landsat images. The estimation of land surface emissivity (LSE) is also required to estimate LST since LSE is a proportionality factor that scales the black body radiance (Planck's law) to measure emitted radiance. Therefore, the NDVI threshold method was used to estimate the emissivity of different land covers, as suggested by Jeevalaxmi (2017). Finally, LST was retrieved using Equation 3.

$$LST = [BT / (1 + (\lambda * BT / \rho))] * \ln(\epsilon) \quad (3)$$

where LST is in Celsius (C), BT is at-sensor brightness temperature (in C), λ is the average wavelength of thermal bands, ρ is $(h \cdot c / \sigma)$, which is equal to 1.438×10^{-2} meter Kelvin, σ is the Boltzmann constant (1.38×10^{-23} Joule per Kelvin), h is Planck's constant (6.626×10^{-34}), c is the velocity of light (3×10^8 meters/second) and ϵ is the spectral surface emissivity (Jeevalaxmi, 2017).

3.2 Ground-based Soil Salinity Measurements

One hundred soil samples were collected from different sites in the Sundarbans to validate the accuracy of NDSI estimates (Figure 1). A stratified random sampling technique was used to gather at least one soil sample from each accessible island in the broader Sundarbans area. Due to a legal prohibition on visitor access, soil samples could not be collected from the core area of the Sundarbans Biosphere Reserve. The soil samples were collected intermittently from December 2018 to March 2020. Soil samples were dried, crushed, and sieved through a 2 mm sieve. The electrical conductivity of each piece was measured using an auto-digital conductivity meter.

3.3 Statistical Metrics and Model Validation

The pixel level NDSI-2019 values were compared with soil EC measurements. In the present study, the validation was carried out with the EC values obtained from the

available soil sample locations. This cross-validation provides greater confidence in using remotely sensed-based NDSI to understand salinity in the Sundarbans. The relationships between pairs of environmental indicators were plotted in scatter diagrams and characterized based on linear regression estimates. The coefficient of determination (R^2) for these estimates was also calculated with P values at < 0.05 to test the statistical significance of the variables.

4. RESULTS AND DISCUSSION

The various estimated remote sensing-based environmental indicators provide different perspectives for understanding the past and current states of mangrove forests in the Sundarbans. The indices extracted from the study play an essential role in exhibiting the fluctuations of the Sundarbans in response to anthropogenic and environmental changes. Field observations in the intertidal zone of the Sundarbans are often difficult due to frequent inundations. Thus, the study used a satellite imaged-based spectral approach for a better interpretation of the dynamics in the Sundarbans.

4.1 Spatio-temporal Trends in NDVI and LST Estimates

NDVI is one of the most widely used indicators for differentiating vegetative cover from other land surfaces. Estimates of NDVI generated in this study (Figure 3) indicate that there is a decrease in vegetative cover between 1972 and 2022. The war that led to Bangladesh's independence from Pakistan in 1971 significantly increased the number of inhabitants in the Indian portion of the Sundarbans due to the influx of refugees from former East Bengal. According to the Census of India 2011, the population in the broader Sundarbans area increased from roughly 2 million in 1971 to 4.4 million in 2011. The rising population was associated with an increase in the Sundarbans' deforestation rate. During the 1980s, the Government of India enacted laws to protect the forests and restrict human activity in the core and buffer zones of the Sundarbans Biosphere Reserve (Ghosh et al., 2015). Government intervention has imposed limited human activity in the Sundarbans' core and buffer zones. However, despite increased population density since 1971, the extent of SBR has remained more stable.

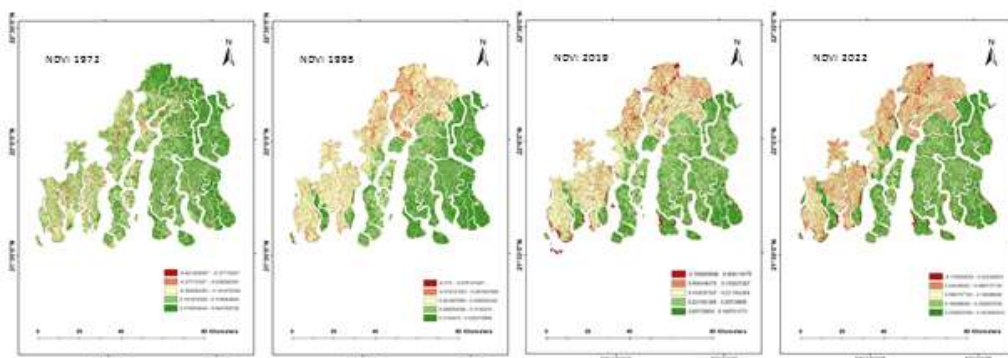


Figure 3. NDVI of 1972, 1995, 2019, and 2022 in the Indian Sundarbans

Deterioration of vegetation health is often associated with frequent and prolonged saline water inundation. The maximum value recorded for the NDVI (0.84) was observed in 1972 and declined to 0.56 in 1995, 0.48 in 2019, and 0.35 in 2022. The decline suggests the loss of dense and healthy mangrove forests. The mean NDVI decreased from 0.23 to 0.14 during this same period.

The relationship between LST and NDVI suggests that declines in surface vegetation cover have been associated with rises in land surface temperature. Areas covered by mangroves showed considerably lower radiant temperatures than non-mangrove areas in 1995 and 2022 (Figure 4). Deforestation driven by increases in population and subsequent economic activity appears to have intensified recent temperature rises. According to the estimates, the maximum LST in the Sundarbans increased by 0.98 °C between 1995 and 2022. The average yearly increase in the maximum temperature observed from 1995-2022 is approximately 0.04° C.

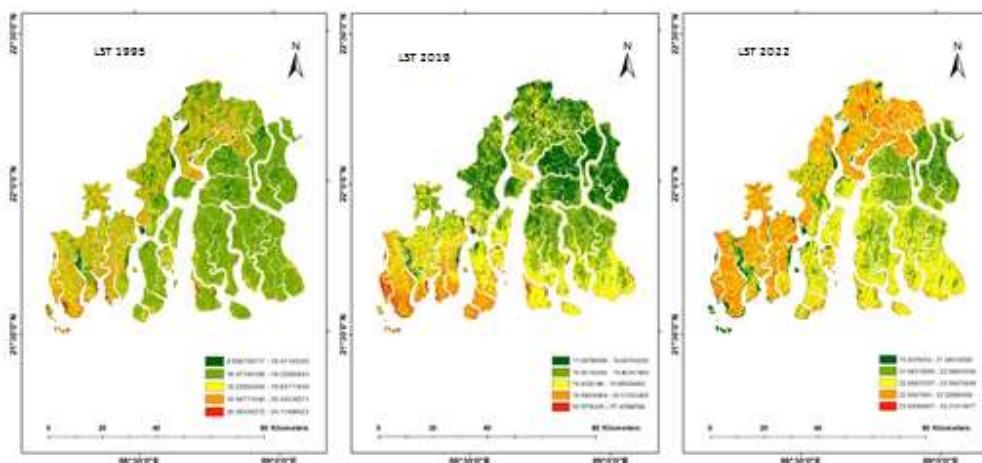


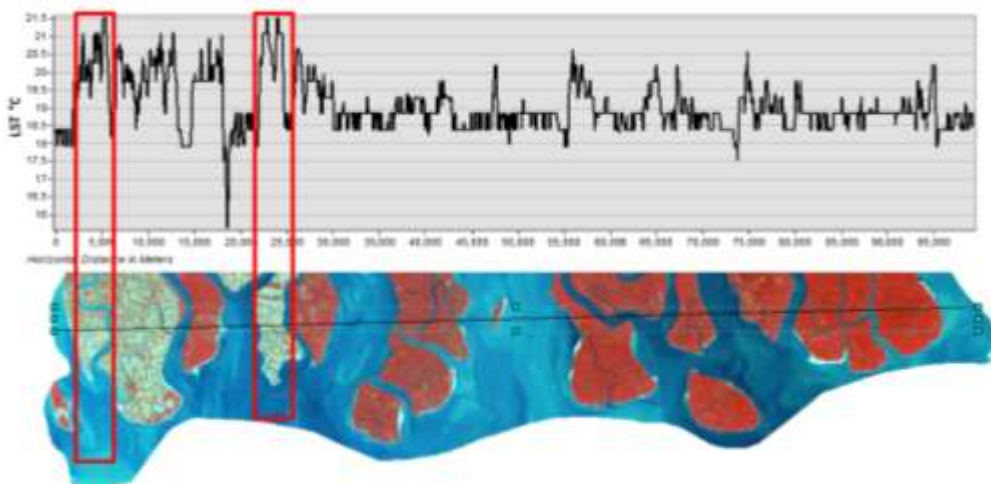
Figure 4. Land Surface Temperature in the Indian Sundarbans during 1995, 2019, and 2022

To understand variations in the increases in LST across the Sundarbans, we compared the differences between estimates made for Henry Island (located on the Southwest edge of the Sundarbans) and the *Burirdabri* area (in the Northeast portion, near the Bangladesh border) of the Indian Sundarbans. The estimated maximum LST in both *Henry Island* and *Burirdabri* show increasing trends, while NDVI estimates show a decreasing trend between 1995 and 2022. As shown in Figure 3, this is consistent with our finding that land without vegetation experienced more significant increases in surface temperatures, i.e., the eastern part of the Sundarbans is covered with relatively dense vegetation (mostly mangroves) compared with the western and southwestern parts.

Furthermore, Figure 5 exhibits that the two spots tracked in the southwestern islands of Sundarbans showed temperatures above 21°C in 1995. In 2019 and 2022, the south-central and northern parts of the island also exhibited a higher temperature (i.e., >21

°C). Hence, our study suggests that forest areas showed gradual and steadily increasing temperatures, suggesting that higher temperatures are not limited to human settlement areas. The reasons are the increased sea surface temperatures, the presence of sand/beach areas, and the degradation of healthy mangroves.

a) 1995



b) 2022

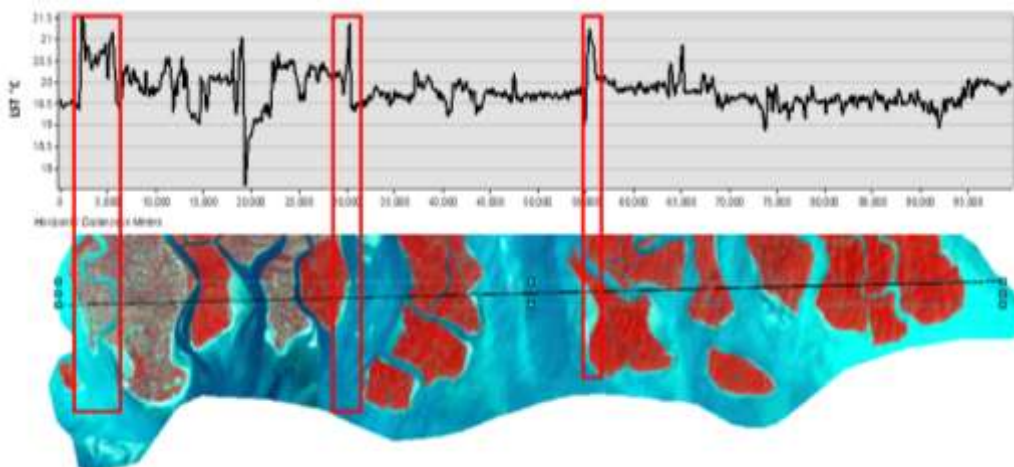


Figure 5. West–East Transect Profile of LST estimates a) 1995 and b) 2022 in the Sundarbans derived from Landsat Data

We generated scatterplots and calculated a regression estimate to examine the relationship between LST and NDVI. These also show that the two indicators are inversely related, both spatially and temporally. A single point change in NDVI is associated with a 3.48 °C decline in LST; the estimated R^2 was 0.267 (Figure 7).

Areas with vegetation frequently inundated by tidal flows display lower temperatures than areas with less vegetation. In comparison, upland areas lacking vegetation generally had higher temperatures. Forests adjacent to settlement zones showed higher temperature fluctuations compared to the interior, less populated parts of the Sundarbans. Estimates indicate that partially deforested islands, cultivated land, fallow lands, and human settlement areas tend to display more significant temperature fluctuations.

4.2 Relationship Between NDVI and NDSI

Salinity is essential in defining species' spatial distribution, assemblage, and density in deltaic mangrove forests. Most of the mangrove genera and families tend to be highly diversified. They have developed specific morphological, biological, physiological, and ecological characteristics that promote adaptability for thriving in the tidal environment (Giri et al., 2014). Soil salinity, present in excessive or insufficient quantities, is a limiting factor in determining the distribution and composition of mangrove species (Mitra et al., 2010). The NDSI is considered a good indicator for identifying salinity-stressed areas. However, relative to NDVI, NDSI is less widely used for mangrove studies. Since the highest salinity is reflected in water bodies, water bodies are removed from our estimates of NDSI. The findings are derived from the pixel values estimated from the islands' interior parts and lands affected by regular tidal flows.

Mangrove species that are highly tolerant of salinity are found in coastal tidal zones, while less tolerant species thrive in the interior parts of the islands. Less tidal water penetration and infrequent and less extreme seasonal inundation in the inland areas account for the lower soil salinity. High NDVI values (i.e., values near +1) indicate healthy vegetation, while NDSI (i.e., values near +1) indicate high salinity. NDSI reported in Figure 6 suggests that the various mangrove species regulate the salinity profile in densely forested areas. In contrast, the areas of greater human habitation display higher soil salinity levels, devastatingly affecting soil fertility and agricultural productivity. Orange- and red-tinted areas in Figure 6 indicate areas of high salinity corresponding to human settlement areas. These areas are concentrated in the northwest of the study area. Moreover, small pockets of highly saline soils are scattered across the Sundarbans and correspond to shallow, frequently inundated mangrove areas, where high evapotranspiration rates lead to high salinity.

Rising soil salinity will cause the agricultural areas to become unproductive, thus negatively affecting the economic conditions where most of the population depend on agriculture for their livelihoods. Moreover, blending sea water with the salty water found in mangrove swamps will have disastrous impacts on the health and biodiversity of the Sundarbans' mangroves. This study has found that the mean NDSI values increased from -0.24 in 1972, -0.21 in 1995, to +0.17 in 2019, and +0.19 in 2022 (Figure 6). Figure 7 suggests a moderate negative correlation between NDVI and NDSI values, suggesting that high salinity is inversely related to vegetation (with $R^2 = 0.533$ and $p\text{-value}=0.43$). Mangrove

species' spatial distribution and growth depend on the salinity profile at different topographical gradients. The relationship between estimated values of NDSI and NDVI varies spatially over the Sundarbans area (aside from the general relationship found in this study).

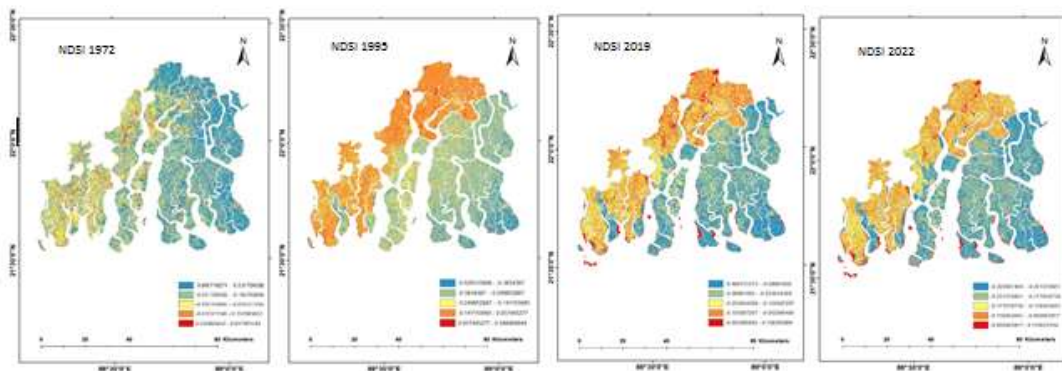


Figure 6. NDSI of 1972, 1995, 2019, and 2022 in the Sundarbans

4.3 Soil EC and NDSI Comparisons

In contrast to other tropical forests, where salt concentrations and variations are low, soil salinity in the deltaic zones fluctuates highly due to daily tidal activity and salt accumulation in the soil, producing a crucial salinity change that affects the spatial distribution of mangrove species. Joshi and Ghose (2003) showed that soil salinity tends to decrease from the tidal coast to the interior of the Lothian islands. The present study focuses on the analysis of soil salinity using both remote sensing techniques and conventionally measured soil EC.

EC offers a rapid, reliable, and easy measure of the number of dissolved ions (total dissolved species, TDS) in the soil solution (dS/m) and measures the ability of the water suspension to conduct electricity; higher salt concentrations to work more current (Corwin and Yemoto, 2017). EC and the total salt concentration of a soil solution are closely related by applying a simple conversion standard (depending on soil type). According to Sahana et al. (2020), the measured EC of the soil samples was highly correlated to the satellite-derived NDSI compared to other salinity indices. Abdul-Qadir et al. (2010) also found that the visible red band performs best among the Landsat bands for characterizing the pattern and features of soil salinity due to its high correlation with measured EC.

However, the accuracy of estimates declines when raster values are compared with corresponding ground location points where the topographical gradient varies significantly. It is likely because the exposed coastal areas subject to daily inundation of tidal flows are often misrepresented as water pixels in satellite imagery. This study overcame this challenge by comparing remote-sensed indicators to field data temporally and spatially. Field observations have potential uncertainties because sites that undergo daily inundation

are challenging to recognize in satellite imagery. In most cases, such areas appear as water pixels or bare mudflats with no vegetation.

The soil salinity was validated by comparing remote-sensed NDSI to measured soil EC. There is a high correlation between NDSI and measured EC of 0.601 (with p-value=0.00) (Figure 7). Our study's soil salinity measurements in coastal areas with daily inundated tidal flows found high soil salinity in remotely sensed data (NDSI). This was confirmed when compared to EC values from soil samples in the inhabited/accessible areas of the Sundarbans.

Based on the spatial location and distribution of EC points, corresponding values of NDSI (generated from Landsat 2019) were plotted on a scatter diagram (Figure 7). Regression of the NDSI and EC measures shows a moderately high positive trend (a one-point increase in NDSI is associated with a 20.7 MHOS/cm increase in EC) with an R^2 of 0.601 and p-value of 0.001. Two islands in the interior of the Sundarbans—*Panchmukhani* and *Khatuajuri*, showed higher values in measured EC (12.71, 13.91) and satellite-derived NDSI (0.38 and 0.30), respectively. The reason may be their interior location along tidal channels with minimum dilution with the freshwater from other creeks and channels.

4.4 Relationships Between Environmental Indicators

Our study found that there is a relationship between LST, NSDI and NDVI across the Sundarbans. In general, increasing soil salinity levels appear to alter the distribution and growth of mangrove species directly. Estimates of the statistical relationships between NDVI-NDSI, NDSI-EC and NDVI-LST explain such spatial variabilities of the mangrove ecosystem in the study area (Table 2). Based on this study's estimated changes in vegetation, salinity, and temperature in recent decades, it is inferred that the mangrove forests in the Sundarbans are undergoing constant changes in terms of the composition of species due to rises in soil salinity and temperature, erratic rainfall, frequent flooding, and increasingly severe storms (Das et al., 2021).

Table 2. Descriptive Statistics of Spectral Indices (LST, NDSI, and NDVI) and Measured E.C.

INDICES	REGRESSION EQUATION	SAMPLE NUMBER	R^2	STANDARD ERROR	P-VALUE (INTERCEPT)
NDVI- LST	$y=19.54 - 3.477x$	160	0.267	0.709	0.00
NDVI- NDSI	$y=0.009 + 0.682x$	160	0.533	0.085	0.43
NDSI- EC	$y=9.074 + 20.66x$	100	0.601	1.482	0.00

[Significance level: $p < 0.05$]

Overall, these changes are increasing the vulnerability of the Sundarbans. In the southwestern and northern portion of the study area, where human settlement is relatively dense, mangroves are relatively scarce, and vegetation is less dense. Proximity to human settlements and the degradation of mangrove forests due to anthropogenic activities likely contributed to the relatively high temperatures observed in these areas in 1995, 2019, and 2022. The discussions with the local respondents during the field visits confirmed that these locations were once densely forested and have now been converted to human settlements with intensive agricultural activity.

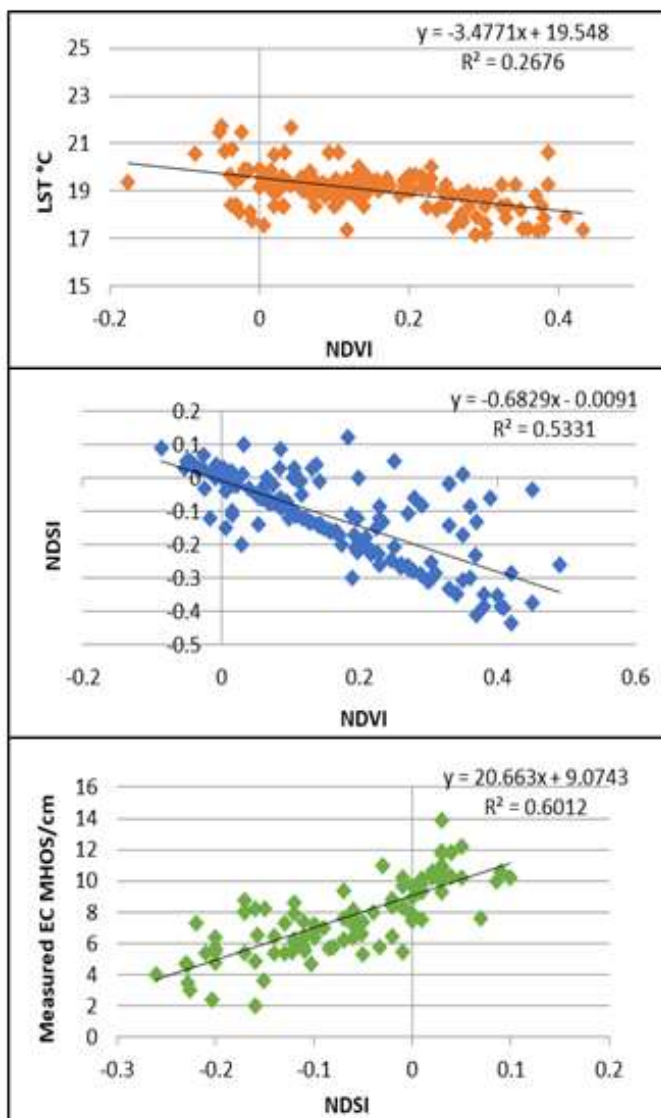


Figure 7. Scatter plots showing the relationship between spectral indices (i) NDVI-LST (ii) NDVI- NDSI (iii) NDSI-Measured EC

5. CONCLUSION

The remote sensing-based spectral analysis shows increased surface temperature and salinity over the period, while the vegetation cover decreased remarkably from 1972 to 1995. However, the net forested areas remained the same due to government policies, but the quality of the mangroves deteriorated over time. Overall, the spectral reflectance of

vegetation decreased by 6.19% from 1972-2022. The average surface temperature across the Sundarbans has increased by 14.9%, both in the human habitat and the mangrove zones. The salinity of the Sundarbans has also increased, and the abrupt increases in salinity have reduced the growth of less saline-resistant mangrove species, suggesting that salinity causes changes in species types and assemblage. The accelerating increase in salinity affects the spatial distribution of mangrove species along the topographical slope but not the density. The high salinity tolerant mangrove species tend to grow in the more frequently inundated newly formed islands spotted during our field survey. Moreover, the eustatic mean sea level and the frequency of storms and cyclones have increased the severity of saltwater intrusions in low-lying arable coastal parts of the Sundarbans. These factors will not only affect the distribution of mangrove species but also cause land degradation of low-lying inundation lands due to increased salinity, compromising agricultural productivity and the livelihoods of the local inhabitants.

Our study found that the NDSI retrieved from Landsat was consistent with the EC values measured from the soil samples. Hence, NDSI can be used to replicate EC in other coastal areas where changes in salinity play an essential role in shaping local vegetation and its impact on livelihood. Given the importance of the Sundarbans mangrove ecosystem and the rising risks to mangrove survival and health, this study highlights the areas of rising temperatures (LST), increased salinity (NDSI), and decreased vegetative cover (NDVI) for implementing corrective measures to preserve and protect this important World Heritage site.

Acknowledgement

We are grateful to all the officials of the Sundarbans Biosphere Reserve for permitting us to collect the soil samples from the Sajnekhali Wildlife Sanctuary and Buffer zone. We also wish to thank the Indian Statistical Institute for its constant encouragement and necessary support.

REFERENCES

1. Abdul-Qadir, A.M., Benni, T.J., (2010). Monitoring and evaluation of soil salinity in terms of spectral response using Landsat images and GIS in Mesopotamian plain Iraq. *Journal of Iraqi Desert Studies* 2, 19–32. ISSN: 1994-7801.
2. Alongi, D. M., (2015). The Impact of Climate Change on Mangrove Forests. *Current Climate Change Report*, 1 (30–39). [DOI 10.1007/s40641-015-0002-x](https://doi.org/10.1007/s40641-015-0002-x).

3. Corwin, D., Yemoto, K., (2017). Salinity: Electrical Conductivity and Total Dissolved Solids. *Methods of Soil Analysis 2*: 1-16. DOI: [10.2136/ma2015.0039](https://doi.org/10.2136/ma2015.0039).
4. Das, P., Banik, P. Rath, K.C. and Edmond, C., (2021). Precipitation extremes and anomalies of the Indian Sundarban 1984-2018. *MAUSAM*. 72, (847–858). DOI: <https://doi.org/10.54302/mausam.v72i4.3552>
5. Deng, Y., Wang, S., Bai, X., Tian, Y., Qian, Q., (2018). Relationship among land surface temperature and LUCC, NDVI in typical Karst area. *Scientific Reports* 8 1-12. DOI: [10.1038/s41598-017-19088-x](https://doi.org/10.1038/s41598-017-19088-x).
6. Ganguly, D., Mukhopadhyay, A., Pandey, R. K., and Mitra, D., (2006). Geomorphological study of Sundarban deltaic estuary. *Journal of the Indian Society of Remote Sensing*, 34(4), 431-435. <https://doi.org/10.1007/BF02990928>
7. Ghosh, M. K., Kumar, L., and Langat, P. K., (2018). Mapping tidal channel dynamics in the Sundarbans, Bangladesh, between 1974 and 2017, and implications for the sustainability of the Sundarbans mangrove forest. *Environmental Monitoring and Assessment*, 190(10), 582. DOI: [10.1007/s10661-018-6944-4](https://doi.org/10.1007/s10661-018-6944-4)
8. Ghosh, A., Schmidt, S., Fickert, T., and Nüsser, M., (2015). The Indian Sundarban mangrove forests: history, utilization, conservation strategies, and local perception. *Diversity*, 7(2), 149-169. doi: [10.3390/d7020149](https://doi.org/10.3390/d7020149).
9. Giri, S., Mukhopadhyay, A., Hazra, S., Mukherjee, S., Roy, D., Ghosh, S., and Mitra, D., (2014). A study on abundance and distribution of mangrove species in Indian Sundarban using remote sensing technique. *Journal of Coastal Conservation*, 18(4), 359-367. DOI [10.1007/s11852-014-0322-3](https://doi.org/10.1007/s11852-014-0322-3).
10. Hajra, R., Ghosh, A., and Ghosh, T., (2017). Comparative assessment of morphological and land use/landcover change pattern of Sagar, Ghoramara, and Mousani island of Indian Sundarban delta through remote sensing. *Environment and Earth Observation* (pp. 153-172). Springer, Cham. DOI: [10.1007/978-3-319-46010-9_11](https://doi.org/10.1007/978-3-319-46010-9_11)
11. Intergovernmental Panel on Climate Change (IPCC), (2013). Climate Change (2013): The Physical Science Basis. Contribution of Working Group I to the Fifth Assessment Report of the Intergovernmental Panel on Climate Change. Cambridge University Press, Cambridge, United Kingdom and New York, NY, USA, p.1535.
12. International Union for Conservation of Nature, (2010). Mangrove forests in worldwide decline, <https://www.iucn.org/content/mangrove-forests-worldwide-decline> (accessed DATE).
13. Jeevalaxhmi, D., Reddy, S.N., Manikiam, B., (2017). Land Surface Temperature Retrieval from LANDSAT data using Emissivity Estimation. *International Journal of Applied Engineering Research*, 12 (9679-9687).
14. Joshi, H., Ghose, M., (2003). Forest structure and species distribution along soil salinity and pH gradient in mangrove swamps of the Sundarbans. *Tropical Ecology* 44 (197-206).
15. Kar, N. S., and Bandyopadhyay, S., (2015). Tropical storm Aila in Gosaba block of Indian Sundarban: remote sensing-based assessment of impact and recovery. *Geography Review India*, 77(1), 40-54.

16. Kundu, K., Halder, P., and Mandal, J. K., (2020). Forest Cover Change Analysis in Sundarban Delta Using Remote Sensing Data and GIS. In *Intelligent Computing Paradigm: Recent Trends* (pp. 85-101). Springer, Singapore. https://doi.org/10.1007/978-981-13-7334-3_7.
17. Mallick, J., Kant, Y., Bharath, B.D., (2008). Estimation of Land Surface Temperature over Delhi Using Landsat-7 ETM+. *The Journal of Indian Geophysical Union*, 12 (131-140).
18. Mitra, A., Gangopadhyay, A., Dube, A., Schmidt, A., Banerjee, K., (2009). Observed changes in water mass properties in the Indian Sundarbans northwestern Bay of Bengal during 1980–2007. *Current Science* 971445–1452.
19. Mitra, D., and Karmaker, S. (2010). Mangrove Classification in Sundarban using High Resolution Multispectral Remote Sensing Data and GIS. *Asian Journal of Environment and Disaster Management*, 2(2). doi:10.3850/S179392402010000268.
20. Mondal, B., and Saha, A. K., (2018, June). Spatio-Temporal Analysis of Mangrove Loss in Vulnerable Islands of Sundarban World Heritage Site, India. In *The Annual International Conference on Geographic Information Science* (pp. 93-109). Springer, Cham.
21. Rahman, A. F., Dragoni, D., and El-Masri, B., (2011). Response of the Sundarbans coastline to sea level rise and decreased sediment flow: A remote sensing assessment. *Remote Sensing of Environment*, 115(12), 3121-3128. doi: 10.1016/j.rse.2011.06.019.
- Sahana, M., Rehman, S., Patel, P. P., Dou, J., Hong, H., and Sajjad, H., (2020). Assessing the degree of soil salinity in the Indian Sundarban Biosphere Reserve using measured soil electrical conductivity and remote sensing data-derived salinity indices. *Arabian Journal of Geosciences*, 13(24), 1-15. <https://doi.org/10.1007/s12517-020-06310-w>.
22. Sievers, M., Chowdhury, M. R., Adame, M. F., Bhadury, P., Bhargava, R., Buelow, C., ... and Connolly, R. M., (2020). Indian Sundarbans mangrove forest considered endangered under Red List of Ecosystems, but there is cause for optimism. *Biological Conservation*, 251, 108751.
23. Thomas, J. V., Arunachalam, A., Jaiswal, R. K., Diwakar, P. G., and Kiran, B., (2014). Dynamic land use and coastline changes in active estuarine regions-a study of Sundarban delta. *The International Archives of Photogrammetry, Remote Sensing and Spatial Information Sciences*, 40(8), 133. doi:10.5194/isprsarchives-XL-8-133-2014.
24. Thakur, S., Maity, D., Mondal, I. et al. Assessment of changes in land use, land cover, and land surface temperature in the mangrove forest of Sundarbans, northeast coast of India. *Environ Dev Sustain* **23**, 1917–1943 (2021). <https://doi.org/10.1007/s10668-020-00656-7>